Emission intensities and line ratios from a fast neutral helium beam

J-W. Ahn[a)]
Department of Physics, University of Wisconsin, Madison, Wisconsin 53706, USA

D. Craig,[b)] G. Fiksel, and D. J. Den Hartog
Department of Physics, University of Wisconsin, Madison, Wisconsin 53706, USA and Center for Magnetic Self-Organization in Laboratory and Astrophysical Plasmas, Madison, Wisconsin 53706, USA

J. K. Anderson
Department of Physics, University of Wisconsin, Madison, Wisconsin 53706, USA

M. G. O'Mullane
Department of Physics, University of Strathclyde, 107 Rottenrow, Glasgow G4 0NG, United Kingdom

(Received 14 August 2006; accepted 22 June 2007; published online 24 August 2007)

The emission intensities and line ratios from a fast neutral helium beam is investigated in the Madison Symmetric Torus (MST) [R. N. Dexter, D. W. Kerst, T. W. Lovell, S. C. Prager, and J. C. Sprott, Fusion Technol. **19**, 131 1991]. Predicted He I line intensities and line ratios from a recently developed collisional-radiative model are compared with experiment. The intensity of singlet lines comes mostly (>95%) from the contribution of the ground state population and is very weakly dependent on the initial metastable fraction at the observation point in the plasma core. On the other hand, the intensity of triplet lines is strongly affected by the local metastable state (2^1S and 2^3S) populations and the initial metastable fraction plays an important role in determining line intensities. The fraction of local metastable states can only be estimated by making use of electron temperature (T_e), electron density (n_e), and effective ion charge (Z_{eff}) profiles as inputs to the population balance equations. This leads triplet lines to be unusable for the investigation of their local plasma parameter dependence. The ratio of singlet lines at 667.8 nm and 492.2 nm (I_{667}/I_{492}) as well as the ratio of 667.8 nm and 501.6 nm lines (I_{667}/I_{501}) has been investigated for the dependence on T_e and n_e both theoretically and experimentally. I_{667}/I_{492} shows strong dependence on n_e with weak sensitivity to T_e. Measurements and predictions agree quantitatively within a factor of 2. There has been no ratio of singlet lines identified to have strong enough T_e dependence yet. The ratios are expected to be reasonably insensitive to the variation of Z_{eff}. © *2007 American Institute of Physics*.
[DOI: 10.1063/1.2759191]

I. INTRODUCTION

Measurement of line emission from injected neutral atom beams has been used as a diagnostic tool for plasma parameters. Beam emission spectroscopy (BES) from fast deuterium beam is used to measure density fluctuations in the core and edge regions of tokamak plasmas.[1] Plasma temperature and density at the edge of magnetically confined plasmas are well measured using a thermal helium beam.[2] However, the use of thermal helium beam is limited to the plasma edge because of the small penetration depth of the injected neutral particles.

A fast helium neutral beam has several potential advantages: a reduced beam halo, no fractional energy components, greater penetration than deuterium beams, and possibly more efficient charge exchange donation in certain energy regions. It is being considered as the diagnostic neutral beam species for future machines such as the International Thermonuclear Experimental Reactor (ITER) (Ref. 3) to minimize the activation of the vessel and its components.[4] There have been several theoretical and experimental studies with regard to the use of a helium beam as a diagnostic.[5–7] However, the experience with helium is more limited and there are greater uncertainties in the fundamental atomic data. Among the factors affecting beam attenuation and beam emission intensity is the existence of metastable atoms in the beam and effects of effective ion charge (Z_{eff}) and ion impact. The T_e, n_e, and Z_{eff} profiles also determine the evolution of excited state populations and therefore emission intensities. Fast helium BES has been investigated in the Madison Symmetric Torus (MST) (Ref. 10) as a potential diagnostic for local plasma parameter measurements. After a brief review of fast helium BES operating principles in Sec. II, the experimental apparatus and the measurement technique is explained in Sec. III. Theoretical modeling of the beam emission has been carried out and experimental measurements were compared with the predictions (Sec. IV). The effect of metastable atoms in the beam on the emission intensity is of particular interest in contrast to the thermal helium beam or deuterium BES diagnostics. The line ratio technique is carefully examined and the ratio between singlet lines is proposed to be used to avoid the disturbing effect of

[a)]Present address: Center for Energy Research, University of California–San Diego, 9500 Gilman Drive, La Jolla, California 92093, USA.
[b)]Present address: Wheaton College, 501 College Avenue, Wheaton, Illinois 60187, USA.

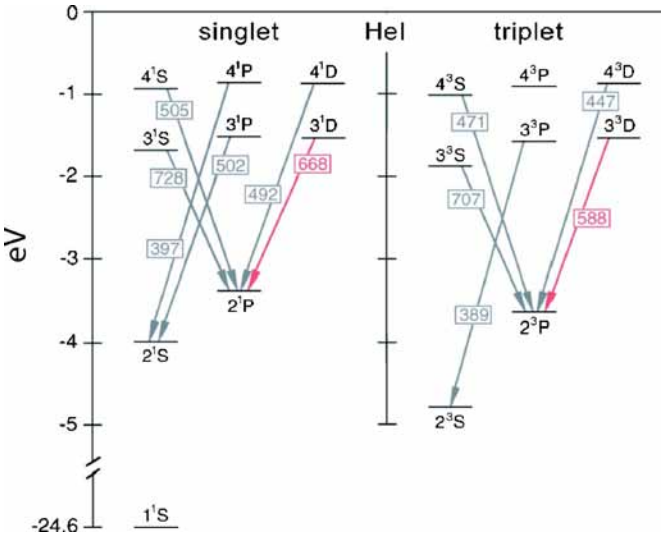

FIG. 1. (Color online) Energy levels of helium with one electron in the ground state, showing some of the allowed transitions (Ref. 11). Numbers in the box represent the wavelength in nm of the emission light corresponding to the transition. The red ones are the most intense singlet and triplet lines among the He I emission lines investigated in this paper.

metastable states. Effects of metastables and the Z_{eff} profile on the He I beam emission as well as on the line ratios are investigated and the results are presented in Secs. IV and V.

II. PRINCIPLES OF FAST HELIUM BES

A. Helium transitions

Helium is an atom with two electrons and hence has two different spin systems, the singlet system (i.e., the spins of the two electrons are antiparallel: $S=\Sigma s_i=0$) and the triplet system (i.e., the spins of the two electrons are parallel: $S=\Sigma s_i=1$). The triplet system can only be populated by spin-changing processes from the ground state, i.e. through electron collisions, whereas the singlet levels are mainly populated by spin-conserving processes from the ground state. The different behavior of cross sections for spin-conserving and spin-changing collisions leads to a rather different temperature dependence of the excitation rate coefficients. In a pure ground state beam, singlet to triplet line ratios are mainly sensitive to temperature. This feature is used to measure the local plasma temperature at the plasma edge with thermal helium beam diagnostics. However the contribution of the metastable population to the beam emission intensity of triplet lines is significant in the case of the high energy beam. Thus the fraction of metastable helium atoms must be known to utilize the temperature dependence of the line ratio for diagnostic purposes. This aspect is discussed in more detail in Sec. IV.

The helium atom has two metastable states, that is, the $1s2s^3S$ (2^3S, triplet) state and the $1s2s^1S$ (2^1S, singlet) state. Figure 1 shows the energy levels for helium with one electron in the ground state. Some of the allowed quantum transitions are shown. Transitions originating from a level with principal quantum number $n>4$ are not considered for emission lines in this paper since the electron population of these higher levels becomes increasingly smaller with increasing n, resulting in weak emission intensities.

Table I shows some selected emission lines in the visible range from the transitions between energy levels given in Fig. 1. These lines have been experimentally investigated and compared with theoretical expectations (see Sec. IV).

B. Statistical balance equations

The fast neutral helium atoms are produced by charge exchange neutralization of He^+ ions during passage through a neutralizing gas cell. Helium atoms become excited by collisions with plasma electrons and ions to a number of higher energy state levels and emit line radiation during deexcitation. A general approach used to obtain the population of energy levels is to find a solution of the statistical balance equations. The statistical balance equations represent the rate at which the excited levels of an atom or an ion are populated and depopulated. In the present work, where we are

TABLE I. He I emission lines selected for the study in this paper. One electron is in the ground state and the other is in an excited state. The beam travel distance $\delta=\nu_b\tau_e$ indicated in the last column is the distance the beam particles progress during the transition time. The beam velocity $\nu_b=8.9\times10^7$ cm/s for the beam energy $E_b=16.5$ keV was used.

λ (nm)	Reference	Transition	Probability (s^{-1})	Transition time τ_e (s)	$\delta=\nu_b\tau_e$ (cm) at $E_b=16.5$ keV
388.9	1^1S	3^3P-2^3S	9.47×10^6	1.06×10^{-7}	9.42
396.5	1^1S	4^1P-2^1S	7.17×10^6	1.39×10^{-7}	12.36
447.2	1^1S	4^3D-2^3P	2.51×10^7	3.98×10^{-8}	3.54
471.3	1^1S	4^3S-2^3P	1.06×10^7	9.43×10^{-8}	8.38
492.2	1^1S	4^1D-2^1P	2.02×10^7	4.95×10^{-8}	4.4
501.6	1^1S	3^1P-2^1S	1.34×10^7	7.46×10^{-8}	6.63
504.8	1^1S	4^1S-2^1P	6.55×10^6	1.53×10^{-7}	13.6
587.6	1^1S	3^3D-2^3P	7.06×10^7	1.42×10^{-8}	1.26
667.8	1^1S	3^1D-2^1P	6.38×10^7	1.57×10^{-8}	1.40
706.5	1^1S	3^3S-2^3P	2.78×10^7	3.60×10^{-8}	3.2
728.1	1^1S	3^1S-2^1P	1.81×10^7	5.52×10^{-8}	4.91

interested in modeling the excited population structure of neutral beam atoms, the statistical balance equations are,

$$\frac{\partial N_i}{\partial t} + \nu_b \frac{dN_i}{dx} = (\text{populating} \rightarrow N_i) - (\text{depopulating} \leftarrow N_i), \tag{1}$$

where ν_b is the beam velocity and dx is along the beam path. The terms in the parentheses on the right-hand side represent the rate at which the atomic processes contribute to populating and depopulating each of the excited levels of the beam atoms, while the terms on the left-hand side include a spatial and time dependent derivative. The spatial derivative represents the rate at which the populations change due to alterations in the local environment as the beam atoms move into the plasma. The time derivative accounts for a change in the population due to a temporal variation in the source of the beam atoms. The neutral beams are considered to be from steady state sources on the time scales of interest and the time derivative of Eq. (1) can be zero, i.e. $\partial N_i/\partial t=0$. It is therefore

$$\nu_b \frac{dN_i}{dx} = (\text{populating} \rightarrow N_i) - (\text{depopulating} \leftarrow N_i). \tag{2}$$

The solution of the above equations yields the population density of each level, N_i.

C. Ranking of atomic lifetimes

The atomic lifetimes associated with the excited levels can vary enormously. However it is possible to separate the excited levels into three distinct categories according to their lifetime.[8] These are autoionizing states with very short lifetimes (τ_a), ordinary excited states with short (radiative) lifetimes (τ_e), and ground and metastable states with relatively long lifetimes (τ_m). Here we consider ground and metastable states under the single classification "metastables." The lifetime of these states, respectively, satisfy the inequality,

$$\tau_a \ll \tau_e \ll \tau_m, \tag{3}$$

where τ_a is $\sim 10^{-13}$ s, τ_e is equal to the reciprocal of the associated transition probability ($\sim 10^{-8}/z^4 \sim 10^{-7}-10^{-8}$ s) and τ_m is $\sim 10/z^8 \sim 10^{-1}$ s, where z is the ion charge. In typical MST plasmas, the time scales on which the local plasma conditions change (τ_p) are in the order of $10^{-3}-10^{-4}$ s. However, the velocity of the beam at the energy of 16.5 keV, $\nu_b=8.9\times 10^7$ cm/s, is high enough so that the flight time for the dimension of the MST, $\tau_f \sim 5 \times 10^{-7}$ s, is much shorter than τ_p and plasma conditions change with the time scale of τ_f in the frame of moving beam atoms. τ_f is comparable to the ordinary excited state lifetimes, that is $\tau_f \sim 5\times 10^{-7}$ s vs $\tau_e \sim 10^{-7}-10^{-8}$ s. In addition, lifetimes of metastable atoms are shortened by collision with plasma particles via ionization and excitation processes. The ranking of the lifetimes is then,

$$\tau_a \ll \tau_e \sim \tau_f < \tau_m. \tag{4}$$

We treat the excited states as being in equilibrium with metastable states, the so-called quasistatic approximation.[9] The statistical balance equation, Eq. (2), should be solved in a spatially dependent manner to obtain the population of "nonequilibrium" metastable states. The population of the excited states is then obtained with respect to the nonequilibrium populations. However, this quasistatic approximation imposes an intrinsic limit on the spatial resolution of the beam emission measurement for a particular transition, coming from the distance traveled in an excited state lifetime. If higher resolution is required, the excited state must be treated dynamically. The beam travel distance for each transition selected for the study in this paper is indicated in Table I. More detailed discussion for modeling is given in Sec. IV A.

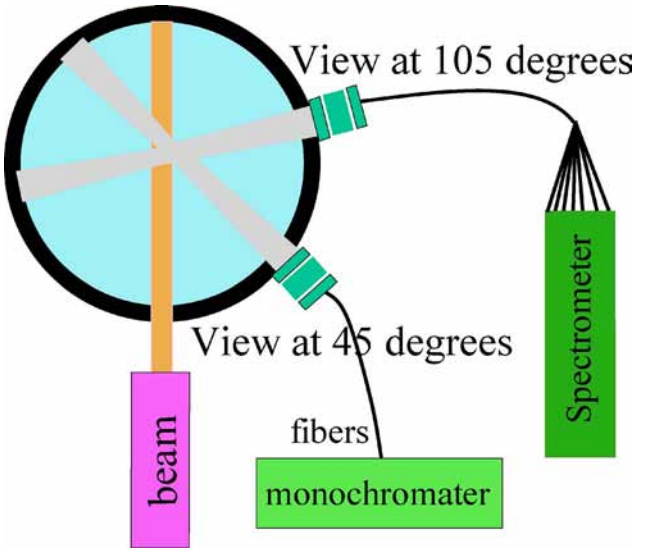

FIG. 2. (Color online) Schematic overview of the diagnostic system employed to measure beam emission intensities, showing poloidal cross section of the system.

III. EXPERIMENTAL APPARATUS

MST (Ref. 10) is a large ($R=1.5$ m, $a=0.52$ m) reversed field pinch (RFP) machine with central electron temperature of up to ~ 2 keV and central plasma density of $0.5-3 \times 10^{13}$ cm^{-3}. The helium neutral beam is fired into the MST plasmas and the beam emission is observed at one spatial point, i.e., at $r/a=0.115$, directly above the magnetic axis ($d=58$ cm along the beam path from entry to the plasma).

Figure 2 shows the schematic overview of the diagnostic system. Two optical heads, with viewing angles of 45° and 105°, collect light from the beam as well as background light. This allows simultaneous measurement of the Doppler-shifted (i.e., redshifted for 45° and blueshifted for 105° viewing angles) helium beam emission light at two wavelengths, enabling continuous (data acquisition frequency of 1 MHz and preamplifier bandwidth of 200 kHz) local line ratio measurements during the beam duration time. Each optical head consists of two measurements; one for beam emission and the other for background light. The background measurement is obtained from a view at the same poloidal location but with toroidal separation of ~4 cm (the beam radius at the

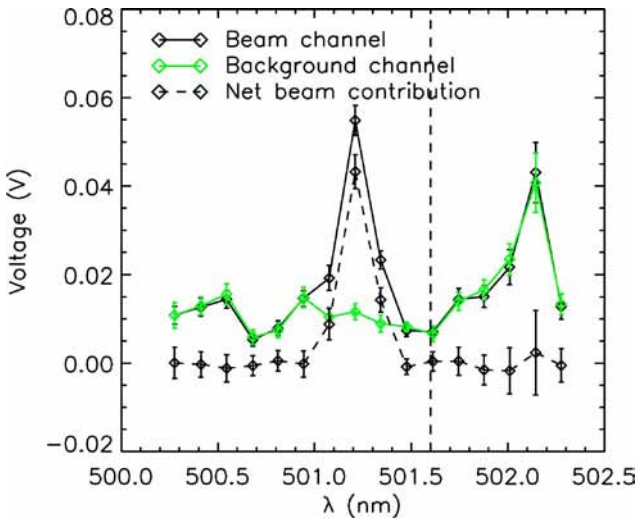

FIG. 3. (Color online) An ensemble averaged, Doppler shifted 501.6 nm He I beam emission line; net beam contribution is represented by the black dashed line, which is the result when the background channel (green solid line) is subtracted from the beam channel (black solid line). The vertical line represents the wavelength of the non-Doppler shifted 501.6 nm He I line.

observation point is ~2.5 cm).[13] The background light is then subtracted from the beam emission view to yield the net beam emission.

The first wavelength (e.g., 667.8 nm He I) is monitored by two grating monochromators with a PMT detector at the exit slit. One monochromator is an f/8.6 Czerny-Turner design with 500 mm focal length (Jarrell-Ash, 1.6 nm/mm dispersion with 1180 g/mm grating). The other is an f/6.5 Czerny-Turner layout with 500 mm focal length (Acton Research, 0.75 nm/mm dispersion with 1800 g/mm grating). The second wavelength (e.g., 492.2 nm or 501.6 nm) is monitored by the Ion Dynamics Spectrometer (IDS) system,[11] an f/10 Czerny-Turner design with 1000 mm focal length (Jarrell-Ash, 0.33 nm/mm dispersion in second order with 1180 g/mm grating). It has 2 input channels and an array of 2×16 output subchannels, each with a PMT detector, to cover a total of ~2 nm wavelength window. In summary, a total of four measurements are employed to simultaneously monitor beam emission and background intensities for two wavelengths of interest.

Figure 3 shows an example of the blueshifted 501.6 nm He I beam emission line, as measured by the IDS spectrometer. The intensity of beam emission is obtained from the integrated area of the net beam contribution. The intensity of the other line (e.g., redshifted 667.8 nm He I), measured by two monochromators, is obtained from the net beam signal multiplied by the wavelength bandpass of the monochromator. A relative calibration of the whole emission detection system was performed for the wavelengths of interest to ensure differences in detector sensitivity were removed.

IV. MODELING A NEUTRAL HELIUM BEAM AND COMPARISON WITH EXPERIMENT

A. Description of modeling

The line emission of fast He atoms in a plasma has been modeled previously by several groups.[5–7] Recently, a collisional-radiative (CR) model for He beams has been developed by the Atomic Data and Analysis Structure (ADAS) group at the University of Strathclyde, Glasgow, UK,[9] which takes into account electron and ion impact excitation, deexcitation, ionization, charge exchange between He and fully stripped ions, and spontaneous emission from excited He states (ADAS 311 and ADAS 313).

The local population density N_i of atoms in state i of a He beam penetrating a plasma can be determined by stepwise solving the steady state balance equations, which can be rewritten from Eq. (2) in matrix form,

$$\nu_b \frac{dN_i}{dx} = \sum_j S_{ij} n_e N_j, \tag{5}$$

where S_{ij} is called the CR matrix, which includes all the collisional and spontaneous emission contributions mentioned above, ν_b is the beam velocity and the quantity dx is along the beam path. The matrix elements S_{ij} are functions of electron and ion temperature (T_e, T_i), electron and ion density (n_e, n_i), effective ion charge (Z_{eff}), and beam energy (E_b). ADAS 311 assembles the balance equations up to an arbitrary principal quantum number n. Levels up to an adjustable threshold n' are treated as *nlSL-resolved* and levels with $n>n'$ are treated as *nS-resolved*, i.e., levels with the same principal and spin quantum number are merged. In our calculations n' was chosen to be 5, the maximum principal quantum number n was 110.

In principle, the statistical balance equations, Eq. (5) could be solved including levels up to an arbitrary principal quantum number n. ADAS population codes allow arbitrary separation into dynamic level populations (described by effective ionization and recombination coefficients for nonequilibrium models) and quasistatic level populations. The metastable separation for the basic use for beams has been employed in the current ADAS beam calculation. One could equally take all $n=2$ and $n=3$ levels as dynamic and higher levels $(n\geq4)$ as quasistatic for short spatial lengths. By far the poor quality of ion collision cross-section data for excited states in helium and the lack of the more correct differential cross-section data in a motional-Stark picture have not warranted this degree of effort. The aim of the first ADAS calculations was to predict expected line intensities in order to assess an initial metastable content and the minimum beam intensity for first experiments for fusion machines. For this purpose a simplified version of the CR model was created by the ADAS group[9] where the excited states are treated as being in equilibrium with the ground state (1^1S) and the two metastable states $(2^1S$ and $2^3S)$ and the equilibrium populations relative to the three nonequilibrium states are obtained.

To calculate the three nonequilibrium level populations $(1^1S, 2^1S$, and $2^3S)$ a set of coupled equations using the CR cross coupling coefficients is constructed. The cross coupling coefficients take into account the influence of stepwise atomic processes. For example the cross coupling coefficient which describes the rate at which the helium 2^3S metastable is populated by the helium 1^1S ground state will include the influence of all possible reaction pathways rather than just the rate for direct excitation. The coupled equations are of the form,

$$\nu_b \frac{dN_{1^1S}}{dx} = -n_e S_{1^1S} N_{1^1S} + n_e S_{2^1S\to 1^1S} N_{2^1S} + n_e S_{2^3S\to 1^1S} N_{2^3S},$$

$$\nu_b \frac{dN_{2^1S}}{dx} = n_e S_{1^1S\to 2^1S} N_{1^1S} - n_e S_{2^1S} N_{2^1S} + n_e S_{2^3S\to 1^1S} N_{2^3S}, \quad (6)$$

$$\nu_b \frac{dN_{2^3S}}{dx} = n_e S_{1^1S\to 2^3S} N_{1^1S} + n_e S_{2^1S\to 2^3S} N_{2^1S} - n_e S_{2^3S} N_{2^3S},$$

where n_e is the electron density and $N_{n^{2S+1}L}$ is the population of the nonequilibrium state specified by the quantum numbers n, S, and L. The CR cross coupling coefficients are represented by the symbol, $S_{n^{2S+1}L\to n^{2S+1}L}$, where the subscripts specify the initial and final nonequilibrium level. The cross coupling coefficients for which the subscript only specifies the initial state, e.g., $S_{n^{2S+1}L}$, refer to what can be described as the total loss coefficient from the level $n^{2S+1}L$. The total loss coefficient includes the CR ionization rate from the level $n^{2S+1}L$ as well as the contribution to populating the remaining levels. These nine coefficients are called generalized collisional-radiative coefficients (GCRCs). GCRCs for a predefined list of plasma temperatures, densities, and beam energies are provided by the ADAS database. Furthermore, for emission lines of interest the so-called effective beam emission coefficients (EBECs) relative to each nonequilibrium level are defined and calculated. These coefficients enable deduction of the line intensity profiles from the population density profiles of the nonequilibrium levels (see Sec. IV C).

An analysis code was developed to numerically solve Eq. (6) by using GCRCs from ADAS. The inputs for this code are the electron density and temperature profiles, the beam energy, the fraction of beam components (1^1S, 2^1S, and 2^3S) on entry to the plasma (i.e., the "initial" fraction; the fraction evolves along the progress of the beam into the plasma as the beam particles interact with the plasma particles), and the step increment. The code solves the coupled equations while moving in small increments along a spatial grid. The beginning and end of the grid is defined by the electron density and temperature profiles. The size of the increment, dx, was selected after running the program several times to obtain a step size which was small enough to ensure numerical convergence but without hugely increasing the computational time. In addition to evaluating the coupling coefficients at fixed points along the grid, the fourth order Runge-Kutta method employed to solve this equation requires coupling coefficients at intermediate points between the fixed step sizes.

The EBECs, along with the profiles of nonequilibrium populations, are used to calculate line intensities. The intensity of an emission line of a wavelength λ is the sum of contributions from each metastable population, including the ground state, and is given by

$$\begin{cases} I_m^{\lambda} = C_m^{\lambda} n_e N_m \\ I_{\text{total}}^{\lambda} = \sum_m I_m^{\lambda} = I_{1^1S}^{\lambda} + I_{2^1S}^{\lambda} + I_{2^3S}^{\lambda}, \end{cases} \quad (7)$$

where C_m^{λ} is the effective beam emission coefficient defined relative to the metastable state m for wavelength λ and N_m is the metastable population density [obtained by solving Eq. (6)]. Table I summarizes the He I emission lines modeled in this study using the GCRCs and EBECs provided by the ADAS database.

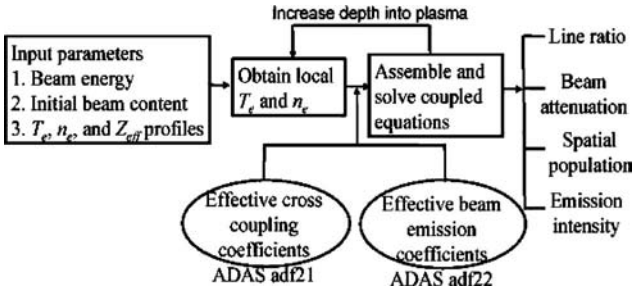

FIG. 4. Schematic illustration of the analysis code employed to solve the coupled equations, which describe the evolution of the ground state (1^1S) and the two metastable populations (2^1S and 2^3S) along the beam. As the input the code requires the beam energy, the fractional metastable and ground state content on entry to the plasma (i.e., the "initial" fraction), as well as suitable electron density, temperature, and Z_{eff} profiles.

The analysis code employs several ADAS library routines to implement the linear interpolation method to assemble the required coefficients at any point along the working grid. A schematic illustration of the code is shown in Fig. 4.

The electron temperature and density profiles were measured by the Thomson scattering and far infrared (FIR) laser systems, respectively, in the MST device. The T_e and n_e profiles fitted to the following equation have been used in the modeling:

$$T_e, n_e\left(\frac{r}{a}\right) = T_e, n_e(0)\left[1 - \left(\frac{r}{a}\right)^{\alpha}\right]^{\beta}. \quad (8)$$

Figure 5 shows an example of such fitted profiles along with experimentally measured temperature and density profiles for an ensemble-averaged "standard" MST plasma (over nine nominally identical standard MST discharges; $I_p = 530$ kA and $\bar{n}_e = 0.5 \times 10^{13}$ cm^{-3}). The Z_{eff} profile is not routinely measured in MST but a recent Bremsstrahlung measurement for plasmas with similar central electron temperature and density indicated[17] Z_{eff} values of 2–3, and therefore a flat profile of $Z_{\text{eff}} = 2.5$ is assumed for the study in this paper. The effect of Z_{eff} profile is discussed in Sec. V A.

B. Estimate of initial metastable fraction

The fast helium beam consists of atoms produced by charge exchange from accelerated ions. These charge exchanged atoms are either in the 1^1S ground state or in one of the two metastable states, 2^1S and 2^3S. The fraction of metastable atoms depends on the gas used for neutralization and its target thickness (line integrated density) in the neutralizer. This initial beam fraction evolves along the progress of the beam into the plasma as the beam particles interact with the plasma particles. The evolution is obtained by solving Eq. (6) in a spatially dependent manner. In order to estimate the initial fraction of metastable atoms a comparison of theoretical modeling with measurement was carried out.

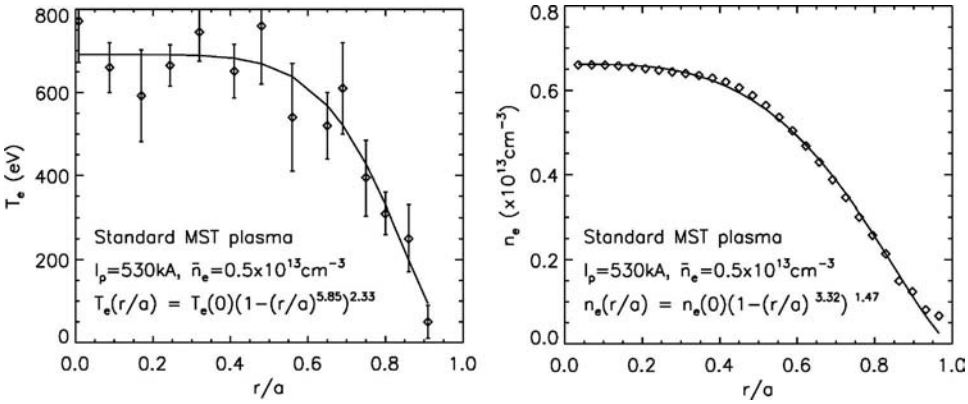

FIG. 5. Measured T_e (by Thomson scattering) and n_e (by FIR) profiles (diamonds) for an ensemble-averaged standard MST plasma with fitting curves (solid lines) to Eq. (8). The fitted $T_e(r/a)$ and $n_e(r/a)$ equations are also indicated. The major radius of the MST is R=1.5 m and minor a=0.52 m. The error bars on the n_e profile data are not provided for this set of data but it is typically estimated that the density data have 6%–10% of error bars, based on the phase measurement error and the error introduced in the numerical inversion process (Ref. 21).

Figure 6 shows the evolution of the intensity of beam emission lines, calculated by the model described in Sec. IV A, with the hypothetical initial metastable fractions of 0% and 3%. 90% of the initial metastable fraction is assumed to be in 2^3S and 10% in 2^1S.[12,19] Additionally, three combinations of 2^1S and 2^3S fractions, that is, 1:9, 5:5, and 9:1, out of the initial 1.2% metastable were tested to calculate singlet and triplet line intensities at the observation point d=58 cm. It is shown that the effect on the three singlet lines used in this paper is minimal while the change in the triplet line intensity is large. This reconfirms that the use of singlet lines for the line ratio technique in the case of high energy helium beam is a better choice than the inclusion of triplet lines.

As all lines of one spin system show rather similar behavior, only the most intense lines of each spin system (667.8 nm for a singlet system and 587.6 nm for a triplet system) are presented in Fig. 6. It is found that the intensity of singlet lines at the observation point (d=58 cm) is very independent of the initial metastable fraction. One can therefore estimate the intensity of a singlet line in the plasma core irrespective of the value of an initial metastable fraction. On the other hand, the intensity of triplet lines is strongly affected by the initial metastable fraction. This implies that the initial metastable fraction must be accurately known to predict the intensity of a triplet line at a particular spatial point.

The strong dependence of triplet line intensity on the metastable fraction can be used to estimate the initial metastable content of the beam. Once the intensities of a triplet line for plasmas with various T_e and n_e values are measured, the ratio of intensities of the line between different plasma parameters can be compared with the theoretically expected values as a function of initial metastable fraction. The best match to experimental measurements gives an estimate of initial metastable fraction. Figure 7 gives an example of such a procedure yielding an initial metastable fraction of 1.2%. Note that the experimental error bar on the 587.6 nm line ratio in Fig. 7 causes uncertainty in the derived initial metastable fraction. However, the resulting variation of initial fraction from ~0.7% to ~3% does not make a noticeable difference in the subsequent analysis results, as only singlet lines have been chosen for analysis in this paper to avoid significant sensitivity to the uncertainty in the metastable fraction at the observation point (see Fig. 6). The initial metastable fraction of 1.2% will be used for all analyses and modeling hereafter.

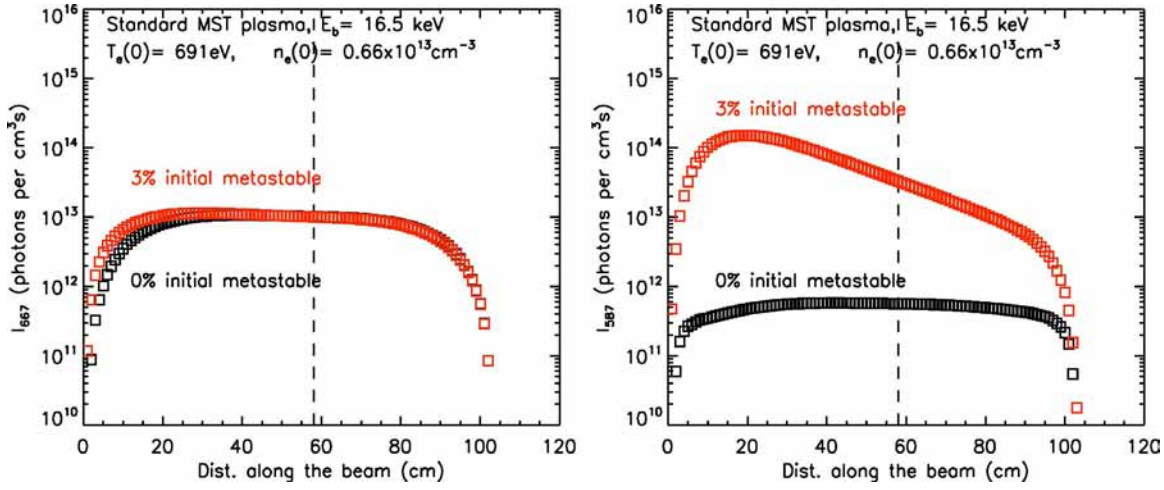

FIG. 6. (Color online) The evolution of the 667.8 nm (singlet) He I line (left) and 587.6 nm (triplet) He I line (right), calculated based on the T_e and n_e profiles in Fig. 5 as well as a flat Z_{eff}=2.5 profile. The black rectangles are based on the beam content of 100% ground state population and on entry to the plasma. The red rectangles are based on 97% initial ground state population. The vertical line represents the point of intersection between the line of sight and the beam path.

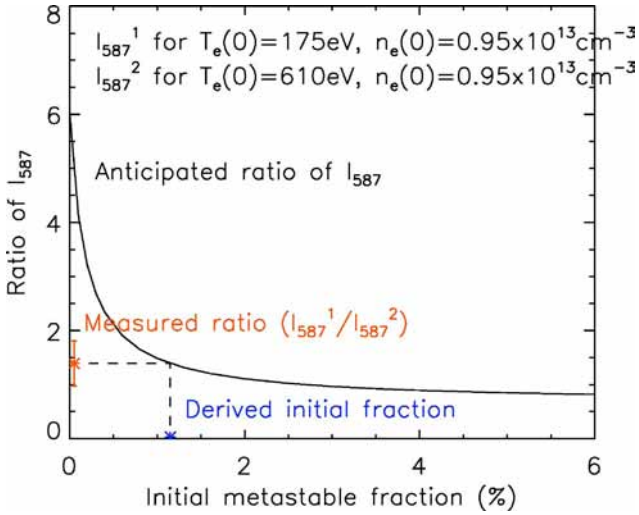

FIG. 7. (Color online) The estimated initial metastable fraction from comparison of the measured ratio of 587.6 nm He I intensity with the theoretically expected values as a function of initial fraction. Note the uncertainty of the estimated fraction due to the error bar on the measured line ratio.

C. Evolution of nonequilibrium populations and emission intensities

The evolution of the three nonequilibrium populations, the spatially dependent solutions of Eq. (6), with the beam energy of 16.5 keV, is shown in Fig. 8. The initial metastable fraction of 1.2% obtained in Sec. IV B was used as an input to the modeling as well as the T_e and n_e profiles shown in Fig. 5 and a flat $Z_{\text{eff}}=2.5$ profile. The populations are relative to the total beam density on entry to the plasma. The total beam density on entry to the plasma is the sum of the ground state and metastable state populations and is estimated to be $N_b \sim 1.6\times 10^{10}$ cm^{-3}.[13] Also indicated in the plot is the calculated fraction of each population at the experimental observation point, i.e., at $d=58$ cm. It is clearly seen that all three populations are attenuated as the beam propagates through the plasma. The decay length of the 2^3S population with respect to the ground population is much longer than that of the 2^1S state; the relative 2^3S population reaches equilibrium only after traversing nearly the entire plasma cross section, i.e., at $d>90$ cm whilst the relative 2^1S population comes to equilibrium before passing the geometric center, i.e., at $d\sim 50$ cm.

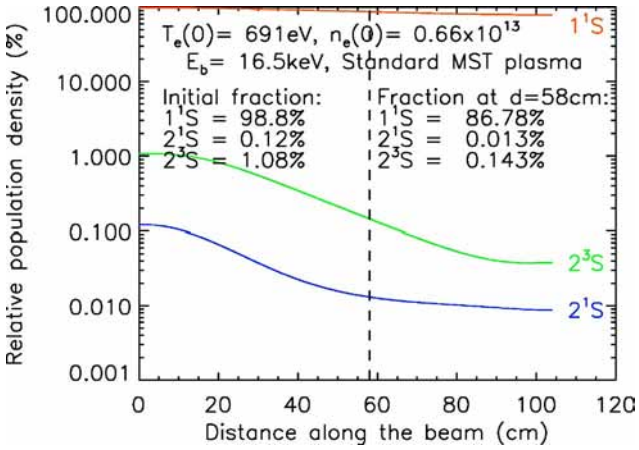

FIG. 8. (Color online) Evolution of the three nonequilibrium populations (1^1S, 2^1S, and 2^3S), relative to the beam density on entry to the plasma, along the fast He beam path in a standard MST plasma (I_p=530 kA, $\bar{n}_e=0.5\times 10^{13}$ cm^{-3}). Calculation is based on the T_e and n_e profiles in Fig. 5 as well as a flat $Z_{\text{eff}}=2.5$ profile. The beam content consists of 98.8% of the ground population and 1.2% of the metastable population, among which 90% 2^3S and 10% 2^1S are assumed, on entry to the plasma. The vertical line represents the point of intersection between the line of sight and the beam path.

The line emission intensity profiles for a total of eleven He I lines in the wavelength range 388.9–728.1 nm (six singlet and five triplet lines given in Table I) were also calculated. Figure 9 shows the emission intensities for a singlet line (667.8 nm He I) and a triplet line (587.6 nm He I) along the beam path. All contributions from the three nonequilibrium populations to the total intensity profiles are shown in the figure.

The total intensity of beam emission for the singlet line contains a significant contribution from metastable atoms (2^1S and 2^3S) at the edge of the plasma but in the core most of the contribution (>95%) comes from the ground state (1^1S). This has an important implication in that the total beam intensity in the plasma core is only weakly affected by the metastable fraction and the total intensity can be estimated to a good approximation by taking account of the ground population only.

On the other hand, the total intensity of beam emission for the triplet line consists mostly of the contribution from the 2^3S metastable state for the whole distance along the beam. Thus the fraction of metastable atoms at a particular spatial point must be known accurately to theoretically estimate the intensity of the triplet line. There is no independent measurement of the metastable fraction at present in MST, therefore it can only be estimated by solving the 3×3 coupled equations [Eq. (6)] with the initial fraction as an input. This requires T_e, n_e, and Z_{eff} profiles, which makes the theoretical estimate of emission intensity at a particular spatial point necessarily dependent on the plasma parameter profiles.

D. Line ratio technique for high energy helium BES

The line ratio technique is widely used in the thermal helium beam diagnostic to measure local T_e and n_e at the plasma edge in fusion devices. It takes advantage of the different behavior of rate coefficients for spin changing (population of the triplet system out of the singlet system) and spin conserving electron collisions. For example, in a pure ground state beam, singlet-to-triplet line ratios are mainly sensitive to the temperature. One important advantage of using the line ratio technique is that it only requires a relative line intensity calibration with respect to the wavelengths of consideration. This is particularly beneficial because currently only one spatial point is available for measurement in MST and therefore it is not possible to obtain emission profiles. For singlet lines, only emission coefficients for ground states are used to obtain line ratios, ignoring the small contributions from metastable states.

For the fast helium beam, metastable atoms in the beam

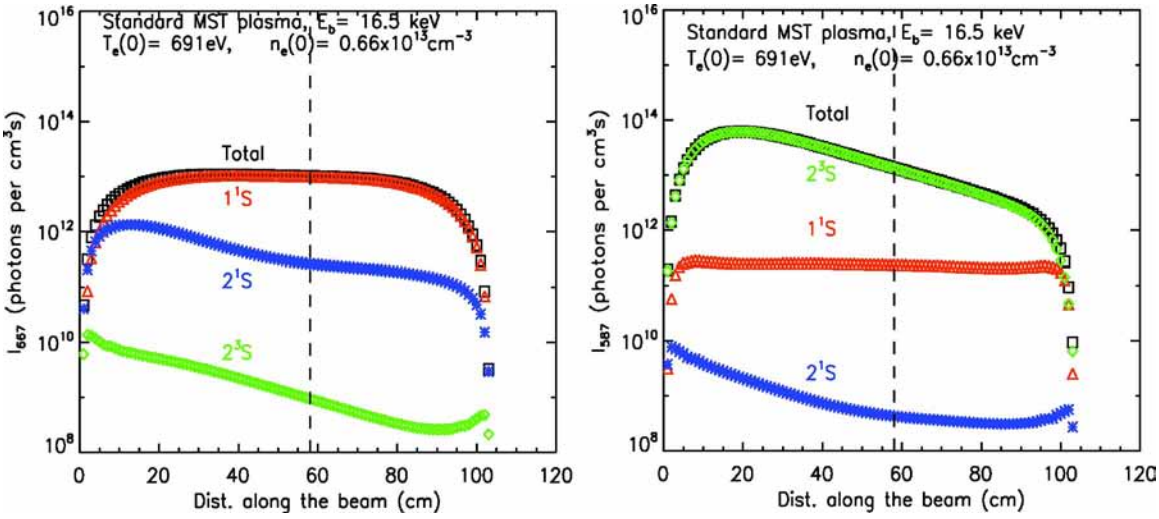

FIG. 9. (Color online) Evolution of the emission line intensities from each of the three nonequilibrium populations ($1^1S, 2^1S$, and 2^3S) along the fast He beam path in a standard MST plasma (I_p=530 kA, $\bar{n}_e = 0.5\times10^{13}$ cm^{-3}) for a singlet (667.8 nm He I, left) and a triplet (587.6 nm He I, right) line. Calculation is based on the T_e and n_e profiles in Fig. 5 as well as a flat Z_{eff}=2.5 profile. The beam content consists of 98.8% of the ground population and 1.2% of the metastable population, among which 90% 2^3S and 10% 2^1S are assumed, on entry to the plasma. The vertical line represents the point of intersection between the line of sight and the beam path.

play an important role. As was discussed in Sec. IV C, the triplet line intensity is strongly affected by the fraction of metastable atoms and this in principle makes the local measurement of plasma parameters impossible with the triplet line ratio unless there is an independent spatial measurement of metastable fraction. However, the line ratio between singlet lines is mostly determined by ground populations. The metastable populations play little role in determining total emission intensities in this case, which makes use of T_e and n_e profiles unnecessary if the small contribution from metastable atoms to the total intensity is ignored. Thus measurement of local plasma parameters is possible to be made if the appropriate dependence of singlet line ratios on the local plasma parameters exists.

The T_e and n_e dependencies of a number of ratios out of six singlet lines in the ADAS database have been theoretically investigated. It is identified that the ratio of 667.8 nm to 492.2 nm He I line intensities (I_{667}/I_{492}) would have a strong dependence on density and a weak dependence on temperature (see Fig. 10). Unfortunately, no excellent ratio with strong temperature dependence has been identified yet in the range of interest. The intensity ratio of 667.8 nm to 501.6 nm He I lines (I_{667}/I_{501}) has dependencies on both temperature and density, except in high T_e and low n_e (e.g., $T_e > 1000$ eV and $n_e < 0.5\times10^{13}$ cm^{-3}) or low T_e and high n_e (e.g., $T_e < 200$ eV and $n_e > 1.5\times10^{13}$ cm^{-3}) ranges, where exclusive n_e and T_e dependence is expected, respectively (see Fig. 10).

E. Comparison of experimental line ratio with theory

The dependence of singlet line ratios on local T_e and n_e was experimentally investigated with data provided by Thomson scattering and FIR systems for the observation point (i.e., at d=58 cm) and was compared with the theoretically expected dependencies. Figures 11 and 12 show the experimental line ratios with the theoretically predicted ratios for comparison.

The general predictions of the modeling are well reproduced by experiment. The measured dependence of I_{667}/I_{492} on n_e is strong, varying from ~3 to ~9 for the density variation from ~0.7 to ~2.0×10^{13} cm^{-3}. A dataset including I_{667}/I_{492} data for similar local n_e values (~1.8×10^{13} cm^{-3}) with different local T_e (~430 eV and ~280 eV, respec-

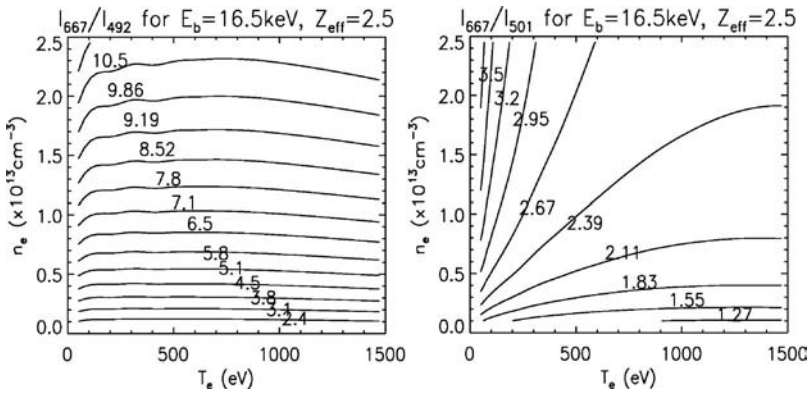

FIG. 10. Contour plots of two singlet line ratios, I_{667}/I_{492} (left) and I_{667}/I_{501} (right). The I_{667}/I_{492} ratio is strongly dependent on the variation of density and shows only very little dependence on the temperature. The I_{667}/I_{501} ratio has dependencies on both density and temperature, except in higher T_e and n_e ranges.

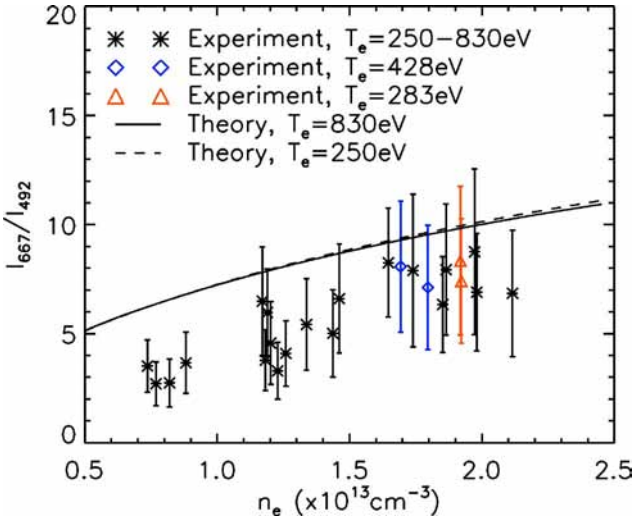

FIG. 11. (Color online) Dependence of I_{667}/I_{492} on the local plasma density. The theoretical line ratio as a function of n_e was calculated for the upper and lower bounds of the experimentally measured T_e values with an assumption of $Z_{\text{eff}}=2.5$ at $d=58$ cm. The theoretically expected insensitivity of the ratio to the temperature was investigated for plasmas with similar local n_e ($\sim 1.8\times 10^{13}$ cm^{-3}) and different local T_e (430 eV for blue diamonds and 280 eV for red triangles).

tively) was taken in order to check the sensitivity of the ratio to the temperature. The data show no clear evidence of I_{667}/I_{492} dependence on the temperature, as is expected by modeling (see Fig. 11).

The dependence of I_{667}/I_{501} on T_e (Fig. 12) is significantly weaker than that of I_{667}/I_{492} on n_e (Fig. 11). This makes the experimental confirmation of the negative T_e dependence of I_{667}/I_{501} more uncertain (the degrees of experimental scatter of the two ratios are similar). Nonetheless, it is notable that the measured I_{667}/I_{501} data have a temperature dependence very similar to that of the theoretically expected ratio. The moderate n_e dependence of this ratio is not well

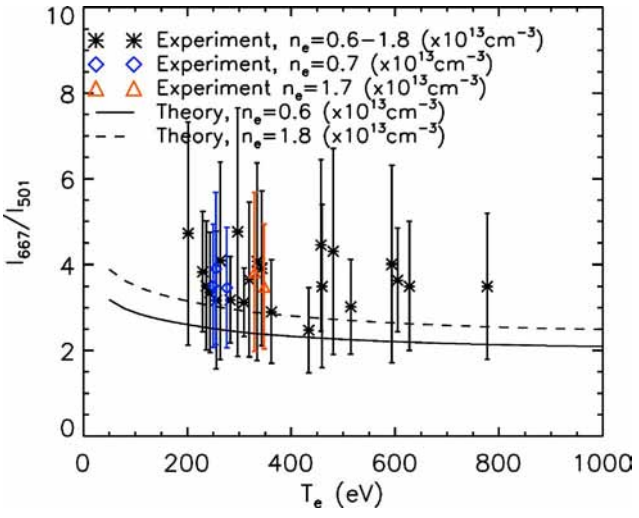

FIG. 12. (Color online) Dependence of I_{667}/I_{501} on the local electron temperature. The theoretical line ratio as a function of T_e was calculated for the upper and lower bounds of the experimentally measured n_e values with an assumption of $Z_{\text{eff}}=2.5$ at $d=58$ cm.

confirmed, due to the relatively higher error bars, by data points with similar T_e($\sim$300 eV) and different n_e ($\sim$0.7 and $\sim 1.7\times 10^{13}$ cm^{-3}).

The quantitative match of theoretical and experimental results for I_{667}/I_{501} is better than for I_{667}/I_{492}. One possible explanation for the larger discrepancy for I_{667}/I_{492} is the effect of magnetic field on the Einstein coefficient for 492.2 nm line, which can be caused by the $n=4$ level mixing between singlet and triplet sides (see Sec. V B for more details) and is not determined in the ADAS311 calculation.

V. OTHER FACTORS INFLUENCING EMISSION INTENSITIES AND LINE RATIOS

A. The effect of Z_{eff} profiles

The beam emission intensity is affected by impurities inside the plasma. As it is impractical to tabulate all possible mixtures of impurities, the usual practice has been to execute ADAS311 in turn for each impurity species treated as a pure species. The mixed species GCRC and EBEC (see Sec. IV A) are constructed by linearly superposing these pure impurity solutions. Although previous error analysis for the deuterium beam[16] indicated relatively small error bars associated with this linear superposition, this can introduce some error bars to the final result. The associated GCRC and EBEC for each impurity as well as for the bulk plasma particles contribute to the beam attenuation and beam emission intensities. The spatial distribution of impurities determines the profile of the effective ion charge, Z_{eff}. There is currently no routine diagnostic for reliable Z_{eff} profile measurement in typical MST plasmas. We have assumed a flat $Z_{\text{eff}}=2.5$ profile in our modeling, based on the result from a recent NIRB measurement in MST.[17] Figure 13 shows the modeling result for various flat Z_{eff} profiles. Singlet lines are less affected by the variation of Z_{eff} than triplet lines. The triplet line intensity at the observation point varies by a factor of $\sim$2 in response to the variation of Z_{eff} from 1 to 2, which indicates the importance of accurate Z_{eff} information for estimating triplet line intensities. Spatial variations in the Z_{eff} profile were also considered, e.g., peaked in the plasma core as was reported by Carraro *et al.*[15] The main features mentioned above remain with some minor changes in the emission profiles. The change is again relatively larger for triplet lines.

Now we examine the effect of Z_{eff} on the singlet line ratio. Figure 14 shows the variation of the two line ratios, I_{667}/I_{492} and I_{667}/I_{501}, as a function of local Z_{eff}. The standard MST plasma shown in Fig. 5 was assumed for the local plasma parameters at the experimental observation point to be used in the line ratio calculation. It is seen that neither of the ratios has strong Z_{eff} dependence, e.g., I_{667}/I_{492} varies from 5.5 to 6 with Z_{eff} variation from 2 to 3. The I_{667}/I_{501} ratio is even more insensitive to Z_{eff} (see Fig. 14). Although it is clear that a more accurate local Z_{eff} value would ensure more accurate calculations, the current Z_{eff} assumption appears to lead to the line ratio predictions with reasonably small error bars, e.g., maximum of $\sim$10% of I_{667}/I_{492} and I_{667}/I_{501} variations for $Z_{\text{eff}}=2.5\pm 0.5$.

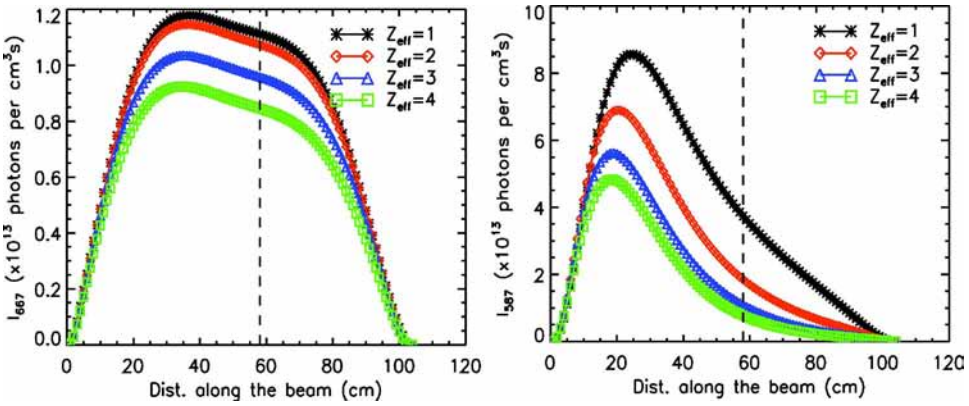

FIG. 13. (Color online) Evolution of emission line intensities along the fast He beam path in a standard MST plasma (I_p=530 kA, $\bar{n}_a$=0.5 $\times 10^{13}$ cm^{-3}) for a singlet (667.8 nm He I, left) and a triplet (587.6 nm He I, right) line. Calculation is based on the T_e and n_e profiles in Fig. 5 as well as flat Z_{eff}=1 to 4 profiles. The beam content consists of 98.8% of ground population and 1.2% of metastable population, among which 90% 2^3S and 10% 2^1S are assumed, on entry to the plasma. The vertical line represents the point of intersection between the line of sight and the beam path.

B. The effect of magnetic field

The separation of helium into singlet and triplet systems starts to break down with the n=4 shell.[18] This is caused by the magnetic field via motional Stark electric field, leading to the effective mixing of the two spin systems. Currently ADAS311 does not have a full calculation of the spin system breakdown, and therefore n=4 level mixing is not determined. The effect of shortened radiative lifetime of the triplet system, acquired from the singlet side via level mixing, is thus not properly estimated. Determination of this mixture requires a full Breit interaction structure calculation.

Indeed the experimental ratio 667/492 is more deviated from the theoretical expectation than 667/501 (Figs. 11 and 12 in Sec. IV E). It is suspected that this might be because of the inclusion of the 492 nm line in the ratio, for which the transition is from 4^1D level and is expected to be susceptible to the B-field effect on the radiative lifetime, therefore on the Einstein coefficient.

The ADAS code is currently not incorporating the effect of reduced Lorentz ionization limit. In our case ($E_b \sim 4$ keV/amu, $B < 0.4$ T), however, any ionization due to the field is from levels above the collisional ionization limit therefore does not seem to be a problem. A report by Janev[20] suggests that it starts at $n > 7$ for E_b=10 keV/amu at 3 T.

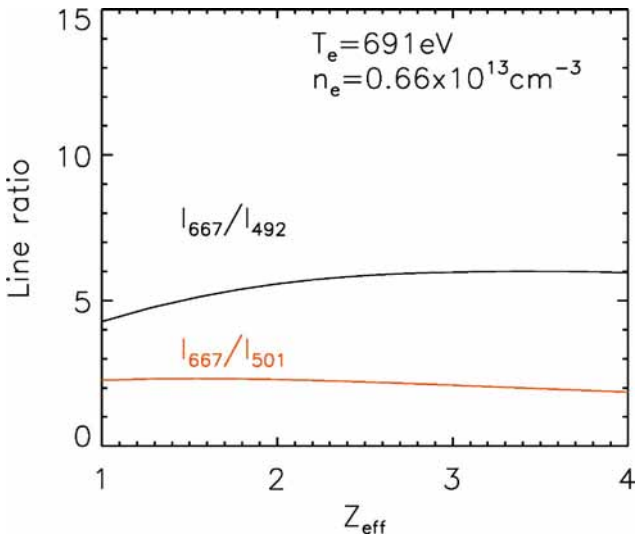

FIG. 14. (Color online) Dependence of local singlet line ratios, I_{667}/I_{492} and I_{667}/I_{501}, on the local Z_{eff} value at the experimental observation point, d=58 cm. The plasma in Fig. 5 is assumed and T_e=691 eV and n_e=0.66 $\times 10^{13}$ cm^{-3} were used as the local plasma parameters for the line ratio calculation.

C. Ion impact effect

In the thermal helium beam diagnostic, plasma ions are considered stationary and play little role in ionizing and exciting beam atoms. In a high energy beam, however, the increased frequency of ion collisional processes due to the high speed of beam particles causes ion processes to become important. The following are the main processes associated with the ion impact:

(i) Single and double ion impact ionization

$$X^{Z+} + \text{He}(1^1S) \rightarrow X^{Z+} + \text{He}^+ + e,$$

$$X^{Z+} + \text{He}(1^1S) \rightarrow X^{Z+} + \text{He}^{2+} + e + e.$$

(ii) Single and double charge exchange

$$X^{Z+} + \text{He}(1^1S) \rightarrow X^{(Z-1)+} + \text{He}^+,$$

$$X^{Z+} + \text{He}(1^1S) \rightarrow X^{(Z-2)+} + \text{He}^{2+}.$$

(iii) Ion impact excitation/de-excitation

$$X^{Z+} + \text{He}(n1^1S) \leftrightarrow X^{Z+} + \text{He}(n^*1^{*1}S).$$

(iv) Transfer double ionization

$$X^{Z+} + \text{He}(1^1S) \rightarrow X^{(Z-1)+} + \text{He}^{2+} + e.$$

The cross sections involved in the ion impact become important for beam energies above several keV.[16] It is therefore clear that the ion impact processes must be properly considered and it is included in the ADAS collisional-radiative model. However, the accuracy of these cross sections is relatively poor as it is difficult to measure or calculate them. The study of error propagation as well as the generation of more accurate ion impact data is being planned by the ADAS group.[14]

VI. SUMMARY AND DISCUSSIONS

The spatially dependent solution of the statistical balance equations determines the evolution of the three nonequilibrium populations (ground state, 1^1S, and two metastable states, 2^1S and 2^3S) for a high energy ($E_b > 15$ keV) neutral helium beam. The excited state populations are assumed to be in equilibrium with these and are expressed relative to the ground state and each metastable state. The effective beam emission coefficients relative to each nonequilibrium state are then defined. This enables the profile of beam emission intensity to be calculated with T_e, n_e, and Z_{eff} profiles as inputs as well as the initial nonequilibrium state content. However, the flight time of high energy beam particles penetrating through the MST plasma is comparable with the transition time of the associated de-excitation processes. This imposes a limit on the spatial resolution of beam emission measurements in the picture of quasistatic approximation, depending on the transition time. It ranges from 1.3 cm to 6.6 cm for the transitions experimentally investigated in this paper for the beam energy of 16.5 keV.

The metastable state atoms in the beam are very important in determining intensities of the triplet He I beam emission lines. A significant fraction of the total intensity comes from contributions from the metastable states and the influence of initial fraction on the emission profile is strong. This implies that the local fraction of metastable populations must be accurately known in order to estimate the local emission intensities. As there is currently no independent measurement of the local metastable fraction in MST, the triplet line is not appropriate as a candidate line for local plasma parameter measurements.

More than 95% of singlet line emission intensity in the plasma core comes from the contribution of ground state atoms. The total intensity in the plasma core is also very insensitive to the initial metastable fraction. Comparison between theory and experiment identified the initial metastable fraction of our beam to be $\sim 1.2\%$. The total intensity can therefore be estimated to a very good approximation by taking account of the ground population only. This makes the singlet line ratio technique useful for the investigation of dependencies on local plasma parameters without knowledge of metastable fraction. A number of singlet line ratios were investigated and the ratio of the lines at 667.8 nm and 492.2 nm (I_{667}/I_{492}) showed good sensitivity to the electron density while the temperature independence was also checked in a moderate level. The ratio between lines at 667.8 nm and 501.6 nm (I_{667}/I_{501}) is expected to have a weak dependence both on the temperature and density in the plasma parameter range of interest. The weak temperature sensitivity is supported by experimental measurement in a range of density variation from 0.6 to 1.8×10^{13} cm^{-3}. An independent measurement of local metastable fraction would allow for the use of triplet lines for the line ratio technique, e.g., the singlet-to-triplet line ratio could be investigated for the local T_e sensitivity study like in the thermal helium beam diagnostic.

The effect of Z_{eff} profiles was also examined. Singlet lines are much less affected by the variation of Z_{eff} than triplet lines. The flat $Z_{\text{eff}}=2.5$ profile assumption for the line ratio calculation causes a maximum of $\sim 10\%$ error in the predicted I_{667}/I_{492} and I_{667}/I_{501} values for the variation of Z_{eff} from 2 to 3. The effect of the magnetic field to cause $n=4$ level mixing is believed to be one of the candidates to explain the larger discrepancy of I_{667}/I_{492} values between theory and experiment than I_{667}/I_{501}. The quality of the ion impact data in helium beam needs to be properly assessed for the error analysis of the subsequent line ratio measurement.

ACKNOWLEDGMENTS

The authors would like to thank the MST scientists and engineers for their support of this project. Special thanks to the Thomson scattering and FIR diagnosticians for the T_e and n_e profile measurements. The authors are grateful to Professor H. P. Summers for helpful discussions.

This work was supported by the U.S. Department of Energy.

[1] G. McKee, R. Ashley, R. Durst, R. Fonck, M. Jakubowski, K. Tritz, K. Burrel, C. Greenfield, and J. Robinson, Rev. Sci. Instrum. **70**, 913 (1999).
[2] B. Schweer, M. Brix, and M. Mehnen, J. Nucl. Mater. **266**, 673 (1999).
[3] ITER Physics Expert Group, Nucl. Fusion **39**, 2137 (1999).
[4] M. G. O'Mullane, H. Anderson, Y. Andrew *et al.*, *Advanced Diagnostics for Magnetic and Inertial Fusion*, edited by P. E. Stott, A. Wootton, G. Gorini *et al.* (Kluwer Academic/Plenum, New York, 2002), p. 67.
[5] F. M. Levinton, Rev. Sci. Instrum. **57**, 1834 (1986).
[6] H. Evensen, D. Brouchous, D. Diebold, M. Doczy, R. J. Fonck, and D. Nolan, Rev. Sci. Instrum. **63**, 4928 (1992).
[7] T. Thorson, R. Fonck, and B. Lewicki, Rev. Sci. Instrum. **70**, 902 (1999).
[8] H. P. Summers, W. J. Dickson, M. G. O'Mullane, N. R. Badnell, A. D. Whiteford, D. H. Brooks, J. Lang, S. D. Loch, and D. C. Griffin, Plasma Phys. Controlled Fusion **48**, 263 (2006).
[9] H. P. Summers, M. G. O'Mullane, H. Anderson *et al.*, Atomic Data and Analysis Structure (ADAS) User Manual, Version 2.6, http://adas.phys.strath.ac.uk(2004), University of Strathclyde, 107 Rottenrow, Glasgow G4 0NG, UK.
[10] R. N. Dexter, D. W. Kerst, T. W. Lovell, S. C. Prager, and J. C. Sprott, Fusion Technol. **19**, 131 (1991).
[11] D. J. Den Hartog and R. J. Fonck, Rev. Sci. Instrum. **65**, 3238 (1994).
[12] M. Proschek, Ph.D. thesis, Technical University of Wien, Austria (2001).
[13] J. C. Reardon, D. Craig, G. Fiksel, and S. C. Prager, Bull. Am. Phys. Soc. **47**, 108 (2002).
[14] M. Proschek (private communications).
[15] L. Carraro, M. E. Puiatti, F. Sattin, P. Scarin, M. Valisa, and M. Mattioli, Nucl. Fusion **36**, 1623 (1996).
[16] H. Anderson, Ph.D. thesis, University of Strathclyde, Glasgow, UK (1999).
[17] M. D. Wyman, B. E. Chapman, S. P. Oliva *et al.*, Bull. Am. Phys. Soc. **51**, 72 (2006).
[18] H. P. Summers, M. von Hellermann, P. Breger *et al.*, AIP Conf. Proc. **257**, 111 (1992).
[19] H. B. Gilbody, W. G. F. Blair, F. R. Simpson, and R. W. McCullough, J. Phys. B **5**, L101 (1972).
[20] R. K. Janev, IAEA Specialists' Meeting on "Required Atomic Database For Neutral Beam Penetration in Large Tokamaks," INDC(NDS)-225/MS (IAEA Nuclear Data Section, Vienna, 1989).
[21] W. Ding (private communications).